agriculture

MDPI

Article

Design and Test of Discrete Element-Based Separation Roller Potato–Soil Separation Device

Xinwu Du [1,2,3,*], Jin Liu [1], Yueyun Zhao [2], Chenglin Zhang [1], Xiaoxuan Zhang [1] and Yanshuai Wang [1]

[1] College of Agricultural Equipment Engineering, Henan University of Science and Technology, Luoyang 471003, China; 220320261813@stu.haust.edu.cn (J.L.); 220320261787@stu.haust.edu.cn (C.Z.); 230320261472@stu.haust.edu.cn (X.Z.); 211430030245@stu.haust.edu.cn (Y.W.)
[2] Longmen Laboratory, Luoyang 471000, China; 230320261501@stu.haust.edu.cn
[3] Collaborative Innovation Center of Machinery Equipment Advanced Manufacturing of Henan Province, Luoyang 471003, China
* Correspondence: du_xinwu@sina.com

Abstract: To address the problems of low bright rates and high rates of potato injuries, a left and right-hand rotation combination of potato–soil separation devices was developed. Its overall structure and working principle were introduced. A Texture Analyzer and pressure sensor were used to measure the force threshold of different varieties of potatoes. A discrete element model of separation rollers and potatoes was established. The collision characteristics of potatoes were analyzed using the device inclination angle, rotational speed, and the center distance of the separation rollers as test factors. A field trial was carried out to optimize the best combination of factors by taking the rate of injured potatoes, bright potatoes, and skin-breaking rate as the test indexes. The force threshold for skin-breaking injury in potatoes was found to be 190–195 N. When the inclination angle of the device was 6°, the rotation speed of the separation roller was 100 r/min, and the distance between the centers of the separation rollers was 79 mm. The rate of injury was 1.25%, the rate of bright potatoes was 99.01%, and the rate of skin-breaking was 1.58%. When the inclination angle of the device was 8°, the rotational speed of the separating roller was 80 r/min, and the center distance of the separating roller was 79 mm, the rate of injured potato was 1.43%, the rate of bright potato was 98.64%, and the rate of broken skin was 1.77%. This paper offers an optimized reference for the effectual removal of sticky soil.

Keywords: agricultural machinery; potato–soil separation; separation rollers; EDEM; loss rate

Citation: Du, X.; Liu, J.; Zhao, Y.; Zhang, C.; Zhang, X.; Wang, Y. Design and Test of Discrete Element-Based Separation Roller Potato–Soil Separation Device. *Agriculture* **2024**, *14*, 1053. https://doi.org/10.3390/agriculture14071053

Received: 7 June 2024
Revised: 26 June 2024
Accepted: 26 June 2024
Published: 29 June 2024

1. Introduction

Potato is one of the crops of strategic importance that has been identified in the world's food security plans [1,2]. As the world's fourth largest food crop after wheat, maize, and rice, it will play an important role in feeding a growing population [3,4]. China boasts a tremendous output of potatoes, but the development of potato harvesting machinery is large but not strong [5–7]. Potato harvesting is constrained by issues such as skin damage, impurities, and injury, which significantly hinders China's potato industry [8]. Only 32% of potatoes were mechanically harvested nationwide, and less than 10% were in in hilly and mountainous areas in early 2022 [9,10]. To increase the mechanized potato harvesting rate and, at the same time, improve the harvesting quality and harvesting efficiency, innovative research on potato–soil separation devices has become urgent [11–13].

To solve the problem of manual potato picking with high labor intensity and low production efficiency, researchers have conducted much research and achieved good application results [14]. Bei Wu et al. [15] divided the potato–soil separation process into five functional areas, namely shearing, bending, throwing, cleaning, and conveying, to determine the key factors of potato–soil separation. Yevhen Ihnatiev et al. [16] studied the process of crushing two neighboring potato beds with vertical rotor blades. Yuyao

Li et al. [17] investigated the working mechanism of the potato–soil separator with rods, analyzed the separation performance of potato pieces and soil, and established a simulation model based on discrete element–multibody dynamics coupling. Wei et al. [18] set up a secondary potato–soil separation device with a vibration separation section and a wave separation section and analyzed the characteristics of the movement of potatoes under the vibration and wave secondary separation conditions. Zhang et al. [19] used multi-stage separation vibration, multiple cushioning, and low side spreading to effectively improve the problems of low rate of bright potato and high damage rate under clay conditions.

At present, the potato harvester potato–soil separation device still has a significant problem. High rates of potato injury and skin breakage can lead to moldy and deteriorating fresh potatoes, making further processing and preparation difficult. If the soil adhering to the surface of the potato is difficult to remove, then a great deal of labor is subsequently required to remove the sticky soil. Low rates of bright potatoes lead to lower potato yields. The research and development of potato harvester potato–soil separation devices is of great significance to the development of the whole potato industry chain.

In this paper, a conveyor separation device combining left-rotation and right-rotation, multi-stage separation, and centralized spreading was designed, which can be adapted to potato harvesting under different soil conditions. The force damage threshold of the potato was determined. The effects of the rotational speed, inclination angle, and spacing of the separation roller on the rate of injured potatoes, bright potatoes, and broken skins were investigated through the kinetic analysis of the soil removal process and the discrete meta-analysis of the potato–soil separation. The soil removal effect of the potato–soil separating device was verified through the field test.

2. Materials and Methods

2.1. Overall Structure and Working Principle

2.1.1. Overall Structure

The potato–soil separating device with separating rollers mainly consists of a left-rotating roller and a right-rotating roller. The left roller rotates to the right, and the right roller rotates to the left when the potato–soil mixture is moving outward. This action moves the potato–soil mixture to the two sides for transport. Conversely, when the potato–soil mixture is moving inward, the right roller rotates to the right, and the left roller rotates to the left. This movement directs the potato–soil mixture to the center for gathering. The overall structure is shown in Figure 1.

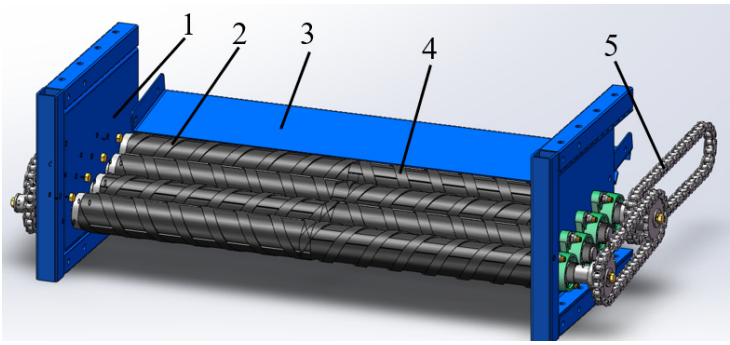

Figure 1. The overall structure of potato–soil separating device: (1) frame; (2) left-hand separation roller; (3) buffer plate; (4) right-hand separation roller; (5) transmission chain.

2.1.2. Working Principle and Main Technical Parameters

Collision and impact during harvesting are one of the main factors causing potato damage and skin breakage [20]. The potato–soil mixture moves from the front buffer plate into the potato–soil separation device with separating rollers. The first separation roller rotates right on the left and left on the right, guiding the potato–soil mixture outward. The secondary separation roller rotates right on the right and left on the left, directing the

mixture inward towards the center. Finally, the last set of rollers performs a combined movement to remove soil after transporting potatoes to the middle, where they fall from the machine. This redesign of the traditional V-shaped structure and reduction in potato collisions during falling reduces the rate of injury to potatoes. The whole device and the horizontal plane are at a certain angle of inclination through the continuous movement of the separation rollers and rotating friction to remove sticky soil.

The main technical parameters of the separating roller potato–soil separation device are shown in Table 1.

Table 1. Separation roller's main technical parameters.

Technical Parameters	Numerical Values
Separation Roller Rotation Speed	80–100 r/min
Pitch of spiral	130 mm
Thread height	5 mm
Device tilt angle	6–10°
Number of left-hand separation rollers	4
Number of right-hand separation rollers	4
Separation roller diameter	72 mm
Number of separation roller stages	4

2.2. Analysis of the Dynamics between the Potato and the Separation Roller

2.2.1. Force Analysis between Potato and Separation Roller

According to the design requirements, the potato should exhibit sliding, rolling, and jumping movements on the separation roller [21]. Potatoes move from the front buffer plate into the potato–soil separation device with separating rollers, where they constantly roll and undergo friction to effectively remove soil. The potato undergoing the separation roller force situation is shown in Figure 2.

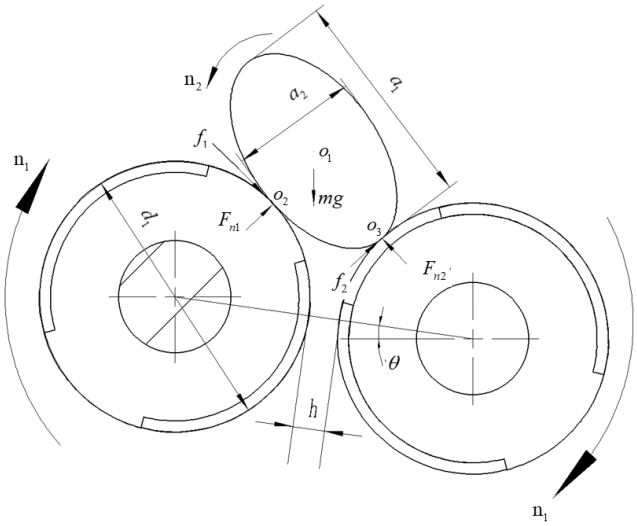

Figure 2. Potato force diagram.

The potato is approximated as an ellipse with the length of the long axis a_1; the length of the short axis a_2; the diameter of the separation roller d_1; the spacing between the two stages of the separation roller h; the inclination angle of the device θ; the rotation speed of the separation roller n_1; the passive rotation speed of the potato n_2; the center of gravity of the potato o_1; and the points of tangency with the separation rollers are o_2 and o_3. The forces on the potato are analyzed, such as its gravity, support, and friction force of the left and right separation roller.

Analysis of the overall continuity of the potato–soil separation device shows that if the potatoes are to be transported backward smoothly and without skin damage, the combined moment of each force acting on the potatoes must be greater than zero [22].

For the convenience of calculation, the coordinate system is established on the graph as follows: the long axis of the potato is the horizontal coordinate x_1, and the short axis is the vertical coordinate x_2, which constitutes the coordinate system x_1y_1. The center of gravity of the potato is the coordinate origin, and the horizontal direction is the horizontal axis x_2, and the vertical direction is the vertical axis y_2, which constitutes the coordinate system x_2y_2. The center of the left separator roller is the coordinate origin, the horizontal direction is the horizontal axis x_3, and the vertical direction is the vertical axis y_3, which constitutes the coordinate system x_3y_3. Furthermore, the angle between the short axis of the potato and the horizontal line is α. Supporting force and the center of the left and right separation rollers constitute the angle of β. The corrected force analysis is shown in Figure 3.

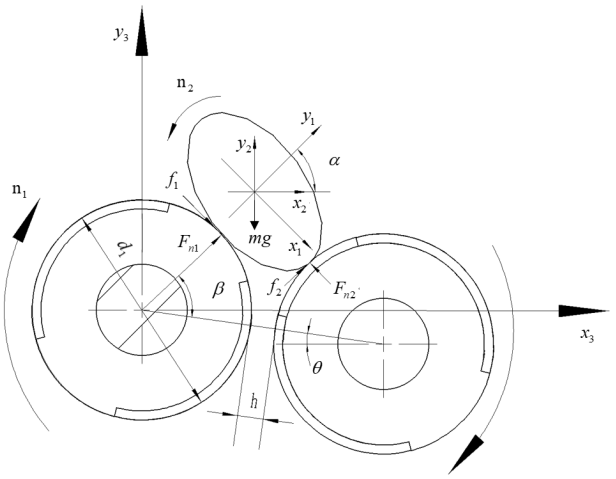

Figure 3. Corrected force diagram.

In the x_1y_1-coordinate system, the approximate elliptic equation of the potato is as follows:

$$\frac{{x_1}^2}{{a_1}^2} + \frac{{y_1}^2}{{a_2}^2} = 1 \tag{1}$$

The equations for the left and right separation rolls in the x_3y_3-coordinate system are as follows:

$${x_3}^2 + {y_3}^2 = \left(\frac{d_1}{2}\right)^2 \tag{2}$$

$$\left[x_3 - \left(h + \frac{d_1 + d_2}{2}\right)\cos\theta\right]^2 + \left[y_3 - \left(h + \frac{d_1 + d_2}{2}\right)\sin\theta\right]^2 = \left(\frac{d_2}{2}\right)^2 \tag{3}$$

d_2 represents the diameter of the right separation roller.

For computational convenience, the equations in the x_1y_1-coordinate systems are transformed into the x_2y_2-coordinate system with the following transformation equation:

$$x_1 = x_2\sin\alpha - y_2\cos\alpha \tag{4}$$

$$y_1 = x_2\cos\alpha + y_2\sin\alpha \tag{5}$$

Then, the elliptic equation of the potato in the x_2y_2-coordinate system is as follows:

$$\frac{(x_2\sin\alpha - y_2\cos\alpha)^2}{{a_1}^2} + \frac{(x_2\cos\alpha + y_2\sin\alpha)^2}{{a_2}^2} = 1 \tag{6}$$

Let the coordinate origin o_1 of the x_2y_2-coordinate system have coordinates (x_0, y_0) in the x_3y_3-coordinate system. Then the potato ellipse equation becomes:

$$\frac{((x_3 - x_0)\sin\alpha - (y_3 - y_0)\cos\alpha)^2}{{a_1}^2} + \frac{((x_3 - x_0)\cos\alpha + (y_3 - y_0)\sin\alpha)^2}{{a_2}^2} = 1 \quad (7)$$

Because the potato and the left and right separation roller are tangential, the change in the potato equation and the separation roller equation simultaneously has a unique common solution. The joint system of equations can be obtained from the point o_1, o_2 in the coordinate system relative coordinates, as follows:

$$\mathrm{x}_{o_1} = \frac{a_1 + a_2 + d_1}{2\sin\alpha}\sin(\alpha - \theta) \quad (8)$$

$$y_{o_1} = \frac{2h\cos\theta}{a_1 + a_2 + d_1}\cos(\alpha + \theta) \quad (9)$$

$$x_{o_2} = \frac{2d_2 h\cos\theta\cos(\alpha + \theta)}{\sqrt{(4h\cos\theta\cos(\alpha + \theta))^2 + (a_1 + a_2 + d_2)^4\sin(\alpha - \theta)}} \quad (10)$$

$$y_{o_2} = \frac{a_1 + a_2 + d_2}{2}\cos(\alpha - \theta) \quad (11)$$

Then, the slope k_1 of the line between the support force F_{n2} and the friction force f_2 can be calculated as follows:

$$k_1 = \frac{[(d_1 + d_2 + h)\sin\theta - (a_1 + a_2 + d_2)\cos(\alpha - \theta)]\sqrt{4h\cos\theta\cos(\alpha + \theta)^2 + (a_1 + a_2 + d_2)^4\sin(\alpha - \theta)}}{(d_1 + d_2 + h)\cos\theta\sqrt{(4h\cos\theta\cos(\alpha + \theta))^2 + (a_1 + a_2 + d_2)^4\sin(\alpha - \theta)} - d_2 h\cos\theta\cos(\alpha + \theta)} \quad (12)$$

Since the directions of the support and friction forces are perpendicular to each other, the product of their slopes is -1, i.e.,

$$k_2 = -\frac{1}{k_1} \quad (13)$$

According to the formula $y = kx + b$, it can also be calculated as, b_1 b_2, respectively:

$$b_1 = (d_1 + d_2 + h)(\sin\theta - k_1\cos\theta) \quad (14)$$

$$b_2 = y_{o_2} - k_2 x_{o_2} \quad (15)$$

According to the formula for the distance from a point to a straight line, the distance s_1 from point o_2 to F_{n2} can be found in turn as follows:

$$s_1 = \frac{|k_1 x_{o_1} - y_{o_1} + b_1|}{\sqrt{{k_1}^2 + 1}} \quad (16)$$

The distance from point o_2 to the line of vector force f_2 is as follows:

$$s_2 = \frac{|k_2 x_{o_1} - y_{o_1} + b_2|}{\sqrt{{k_2}^2 + 1}} \quad (17)$$

The distance from point o_2 to the line of vector force mg is as follows:

$$s_3 = \frac{2h\cos\theta}{a_1 + a_2 + d_1}\cos(\alpha + \theta) - x_0 \quad (18)$$

This gives the combined moment of the individual forces is as follows:

$$\sum M = F_{n2}s_1 + f_2 s_2 + mgs_3 \tag{19}$$

The simplification leads to:

$$F_{n2}\left[(a_1 + a_2 + d_1)^2 \sin(\alpha - \theta) + (d_2 + h)^2 \cos\theta\right] + mga_1 \sin\theta - f_2 h a_2 \cos(\alpha + \theta) > 0 \tag{20}$$

The combined moment equation presented above shows the operation of the potato–soil separation device with separating rollers. The potato and the clay attached to its surface are mainly supported by the separation roller, gravity, and surface friction. The support force is mainly related to the potato's gravity, as well as the separation of the device's tilt angle. Friction is mainly related to the separation of the roller's material, friction coefficient, and support force. According to the formula of the combined torque, the factors affecting the quality of potato de-soiling are the center distance between the separation rollers, the inclination angle of the device, etc. The diameter of the separation rollers was tentatively set at 72 mm, and the spacing of the separation rollers was related to the inclination angle of the device, which was tentatively set at 6°–10°. However, in the actual movement process of the potato and the separation roller collision, friction between the potato collision and the irregular shape of the potato are key factors affecting the quality of soil removal. The actual movement process is more complex [23].

2.2.2. Technical Analysis of the Process of Separation of Clay-Heavy Soils

In response to the problem, harvesting under clay soil conditions in southwestern China often results in half soil and half mud, causing serious difficulties in subsequent transportation and storage [24]. A theoretical analysis of the separation process of potatoes and their surface clay was made to optimize the main parameters of the separation rolls.

According to the Mohr–Coulomb theory [25], the bonding force analysis of the soil adhering to the surface of the potato was performed as a circle. And since the sticky soil was distributed on the surface of the potato, the soil was equated to the curved cross-section of the lower one-fourth of the circle. The force analysis was performed on it. The gravitational forces of the soil block and the potato are, respectively, G_1 and G_2; the interaction forces between the soil and the potato pieces are, respectively, F_1, F_2; the bonding force is F_3, F_4; the interaction force between the potatoes is F_5; the support force of the separation roller on the soil is F_N, as shown in Figure 4.

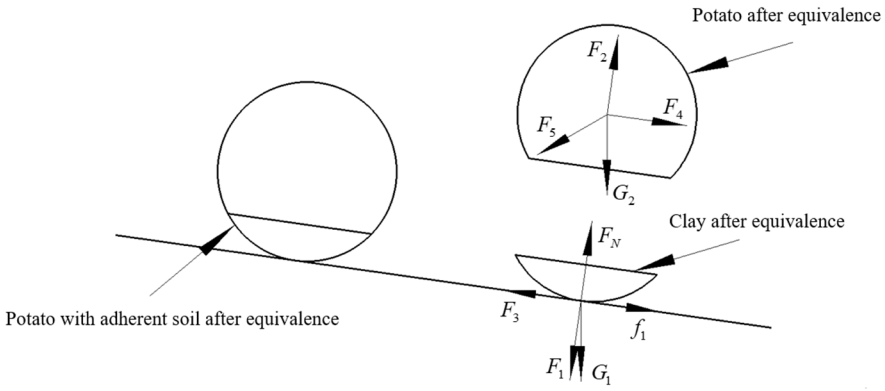

Figure 4. Force analysis of clayey soil separation process.

According to Mohr–Coulomb theory, the soil adhering to the potato surface is mainly separated and destroyed by the action of the shear stress. Through soil destruction tests and comparison of various factors affecting soil breakage, the following formula can be derived:

$$\tau_t = \sigma \tan\varphi + C \tag{21}$$

τ_t is the soil shear strength, kpa; C is the coefficient of soil cohesion; φ is the angle of internal soil friction; σ is the normal stress acting on the crushed surface of the soil, kpa.

The cohesive soil adhering to the surface of the potato has its bonding force calculated by the following formula:

$$F_3 = \tau_t S \tag{22}$$

S is the shear area.

For de-soiling to be effective, the crushing force applied to the soil must be greater than the bonding force between the soils; then, the following can be obtained:

$$f_1 + G_1 \sin\theta > F_3 \tag{23}$$

f_1 is the frictional force on the surface of the potato adhering to the soil.

According to the formula for the bonding force, the average shear force acting on the soil is 8000 N. Since the size of the clay adhering to the surface of the potato is only 300 N per unit area, the component force of gravity in the direction of friction is negligible. It can be concluded that the soil adhering to the surface of the potato can be removed when f_1 meets the force per unit area is greater than 0.8 N. The expression for F_N is as follows:

$$F_N = \frac{mg}{(1-\mu)\cos(\theta+\beta) + (1+\mu)\sin(\theta+\beta)} \tag{24}$$

where the coefficient of friction between the separating roller and the soil attached to the potato surface is 0.9.

From the expression, the friction force on the soil adhering to the potato surface is related to the angle of θ, positively related to the weight of the potato, and negatively related to the sine and cosine values $\theta + \beta$. When the mass of the potato block is 150 g, the inclination angle of the device is 0°, and the minimum value of the friction force can be calculated to be 0.948 N, which is greater than the bonding force of 0.8 N, so that the soil adhering to the surface of the potato can be removed, and the de-soiling work can be completed.

2.3. Measurement of Stress Thresholds in Potato

From the movement of the machine, potatoes continue to roll, and the friction from being thrown up and down produces impact force. If this force exceeds the threshold, the potato experiences skin damage. If the force remains below the threshold, the potato can go through the whole separation process without damage. To reduce the rate of injury to potatoes and ensure the quality of the harvest, it is necessary to measure the force threshold of potatoes to determine under what circumstances skin-breaking damage occurs.

To ensure the reliability of the test results, pressure and impact tests are used to verify and mutually support each other. The pressure test refers to the pressure exerted on the potato by the Texture Analyzer to observe the deformation of the potato as well as the breakage. The impact test refers to the pressure sensor that can measure the real-time peaks. The potato is thrown from a certain height, and then it is tumbled on the platform after the roll, impact, and friction to observe the breakage and record the peak value of the force. The former is complementary, and the latter is the main.

Potatoes were analyzed and tested using several varieties, such as Holland 15, Kexin 1, and Dry Dabai. All three varieties of potatoes are more prone to damage from broken skins than other varieties of potatoes, as shown in Figure 5.

The test apparatus for measuring the compressive capacity of potatoes using a Texture Analyzer is shown in Figure 6. Based on the actual measurements, the forces were finally observed at deformations of 1.5 mm, 2.5 mm, and 3.5 mm.

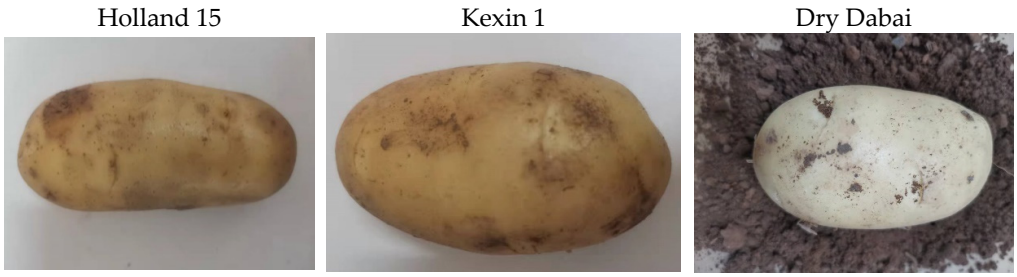

Figure 5. Map of potato varieties.

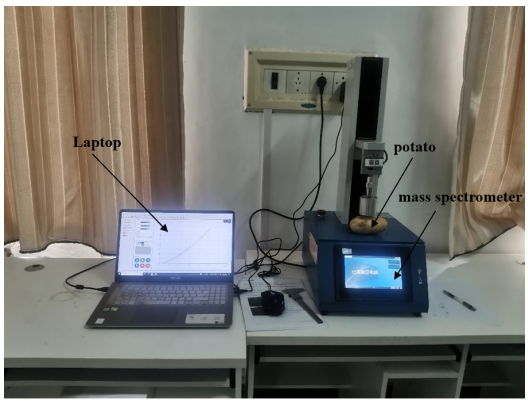

Figure 6. Texture Analyzer.

To test the impact force of the potato filling, a JHHM-H1 pressure load cell was used with peak detection mode. The experimental apparatus is shown in Figure 7. The potato was placed at a certain height above the pressure sensor and was dropped onto it in free-fall motion. For comprehensive consideration, the height of the test in the case of free-fall motion was taken to be 0.5 m, 1 m, 1.5 m, and 1.8 m. The three types of potatoes mentioned previously were used to perform the test. Three sets of tests were repeated at each height.

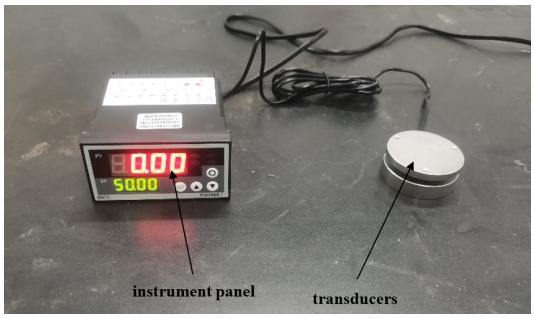

Figure 7. Pressure load cells.

2.4. Discrete Element Modelling

2.4.1. Discrete Element Modelling of Potato and Separation Rolls

To ensure that the potato in the separation device rolls and jumps without incurring skin damage, further analysis of the forces acting on the potato movement is needed [26]. The discrete element method is widely used in agriculture [27,28]. The potato model using the discrete element method is shown in Figure 8 [29]. Potato models are classified as long, ellipsoidal, and spherical, and they describe the shape of the potato as well as possible. The models are all based on polyphase aggregation models. The mass of elongated potatoes is about 205 g, ellipsoidal potatoes about 170 g, and spheroidal potatoes about 150 g. The diameter of long and ellipsoidal potatoes is around 60 mm. Spheroidal potatoes have a diameter of 55 mm.

(**a**) Long.

(**b**) Ellipsoidal.

(**c**) Spherical.

Figure 8. Potato discrete meta-modeling.

The separator rollers are made of natural rubber. The sidewalls of the frame are made of steel plates, and the floor is made of soil. To ensure that the potatoes can be transported smoothly to the potato–soil device with separating rollers, two more stages of separating rollers are set up in front of the device. The pellet factory is set up above it. The established simulation model is shown in Figure 9.

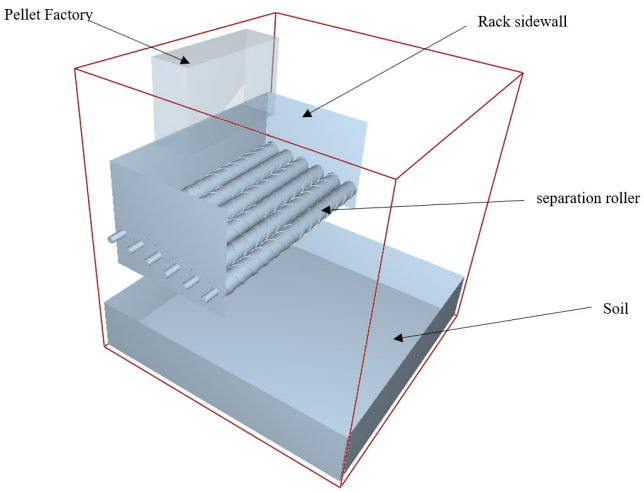

Figure 9. Simulation model diagram.

The rest of the simulation parameters are shown in Table 2.

Table 2. Simulation parameter values.

Parameters	Numerical Value
Poisson's ratio of potato pieces	0.5 [30]
Potato density	1048 kg/m^3
Shear modulus of potato pieces	1.366 Mpa
Coefficient of recovery between plots	0.66
Static friction factor between potatoes	0.452
The factor of kinetic friction between potatoes	0.024
Rubber Poisson's ratio	0.49
Rubber shear modulus	1 Mpa
Rubber density	960 kg/m^3
Coefficient of recovery of collision between rubber and potato	0.7
Coefficient of static friction between rubber and potato	0.5
Dynamic friction factor between rubber and potato	0.4

Separation roller speed, device inclination, and separation roller center distance have a more obvious effect on the damage to the potato. Appropriate rotational speed, inclination angle, and center distance can effectively avoid damage to potatoes in the separation process and prevent the emergence of local blockage and other problems. When the device tilt angle is small, the potatoes continuously roll on the separation roller and are not transported backward. If the device tilt angle is too large, it will lead to the potatoes not being fully rolled and not experiencing friction. Sticky soil can not be completely removed, which may lead to excessive force on the potatoes, increasing the rate of damage. Therefore, the angles of inclination of the device were initially set to be 6°, 8°, and 10°, with each angle corresponding to three speeds of the separator rollers, i.e., 80 r/min, 90 r/min, and 100 r/min. The simulations were analyzed using the maximum force on the particles.

2.4.2. Analysis of the Removal Effect of Clay-Heavy Soils

Separation rollers allow the potato to roll and jump on them, removing the soil adhering to the surface of the potato and avoiding the situation of half potato and half mud when harvesting. Soil particles adhering to the potato surface were established to be 1 mm with a contact radius of 3 mm. Simulation analyses were carried out using the hertz-mindlin with the JKR model.

In the actual harvest situation, the potato is rarely covered by the surrounding soil. However, for better removal of sticky soil, the model soil established in this paper covers about 70–80% of the potato surface. The establishment of the surfaces of the three kinds of potato in the adherent soil model is shown in Figure 10.

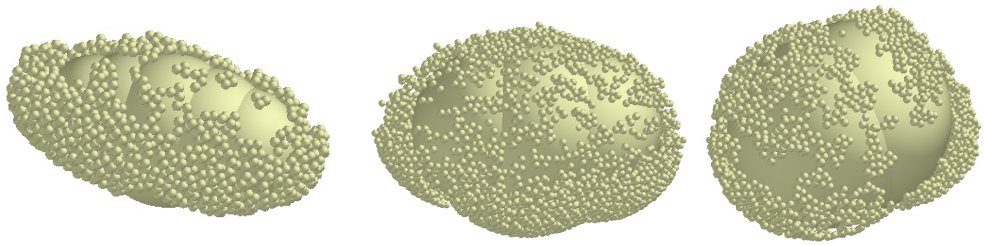

Figure 10. Soil adhesion on potato surfaces.

2.5. Field Trial

The machine is equipped with a 15–20 kw small tractor with an operating width of 900 mm. It has a single-row harvest with a length of 50 m, a width of 400 mm, and a height of 200 mm. The spacing between potato plants in each row is 200 mm. The operating speed is 0.5–1 m/s, and the depth of operation is 120–240 mm.

Based on the above computational analysis of the kinematics of the potato and the simulation analysis of the collision characteristics of the discrete elements, the inclination

angle of the device, the rotational speed of the separation roller, and the center distance of the separation roller were determined as the test factors.

According to the NYT648-2015 Technical Specification for Quality Evaluation of Potato Harvesters [31], the formula for calculating the rate of wounded potatoes e_1, bright potatoes e_2, and skin-breaking rate e_3 as the test indexes is as follows:

$$e_1 = \frac{W_1}{W} \times 100\% \tag{25}$$

$$e_2 = \frac{W_2}{W} \times 100\% \tag{26}$$

$$e_3 = \frac{W_3}{W} \times 100\% \tag{27}$$

W_1 is the wounded potato quality;
W_2 is the quality of bright potatoes;
W_3 is the mass of potatoes with broken skin;
W is the total potato mass.

3. Results and Discussion

3.1. Potato Stress Threshold Test Results

A plot of potato morphology versus pressure tested on a Texture Analyzer is shown in Figure 11.

Holland 15, Kexin 1, and Dry Dabai, the three potato types used, were subjected to the peak force of 179 N, 185 N, and 173 N. Due to pressure, the potato surface did not appear to show obvious abrasion, but the potato flesh was slightly damaged. Compared to other hard surfaces, when the peak force was reached, the potato surface was softened.

The impact of tumbling friction on potatoes falling at different heights using a pressure load cell is shown in Table 3.

Table 3. Measurement results (unit: N).

	0.5 m	**0.7 m**	**1 m**	**1.5 m**
Holland 15	71.2	115.3	141.7	205.3
	64.9	120.1	136.2	197.2
	66.5	113.2	142.6	198.6
Kexin 1	53.7	132.7	137.6	190.8
	55.0	126.1	134.2	197.5
	56.6	123.4	128.4	195.1
Dry Dabai	66.1	118.3	146.1	193.2
	67.5	122.6	134.1	201.1
	71.3	126.7	141.6	197.9

When the test height was below 1 m, i.e., the force on the potato was about 146.1 N or less, no obvious damage to the potato occurred. But, when the impact force was increased to 195 N or more, the potato was damaged to varying degrees, as shown in Figure 12.

After each test, the breakage of the potato was observed. If the potato was already damaged, the value of the impact force at this point was recorded, and the final test result was averaged to about 197 N.

Combined with the damage caused by the above-mentioned Texture Analyzer and the actual situation of the potato moving on the machine, the comprehensive consideration in this paper is that the damage threshold of the potato was set to be between 190 and 195 N. If it exceeded this range, it was recognized as an injured potato.

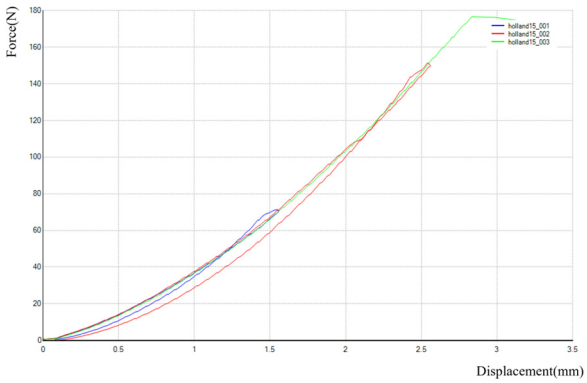

(**a**) Holland 15.

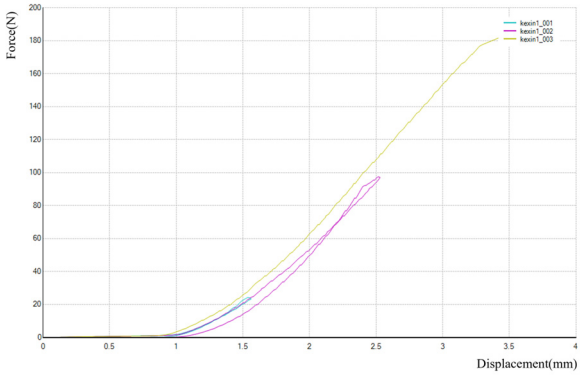

(**b**) Kexin 1.

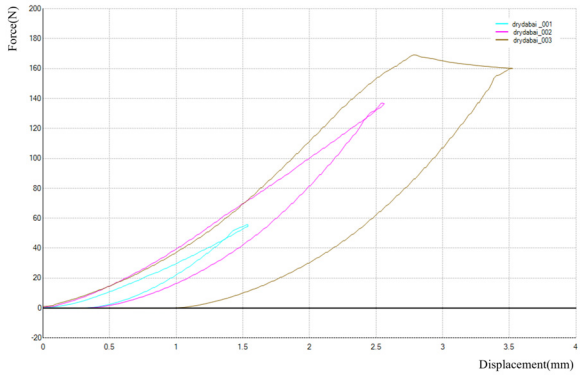

(**c**) Dry Dabai.

Figure 11. Measurement results.

Minor damage Moderate damage Severe damage

Figure 12. Skin-breaking damage in potatoes subjected to forces of 195 N or higher.

3.2. Influence of Device Inclination Angle and Separation Roller Speed on Potato Collision Characteristics

To reduce the degree of damage to the potatoes, it is necessary to ensure that effective shear force can be applied to the soil to break the soil. Figure 13 shows the influence of

different inclination angles and rotational speeds on the mechanical characteristics of the three potatoes.

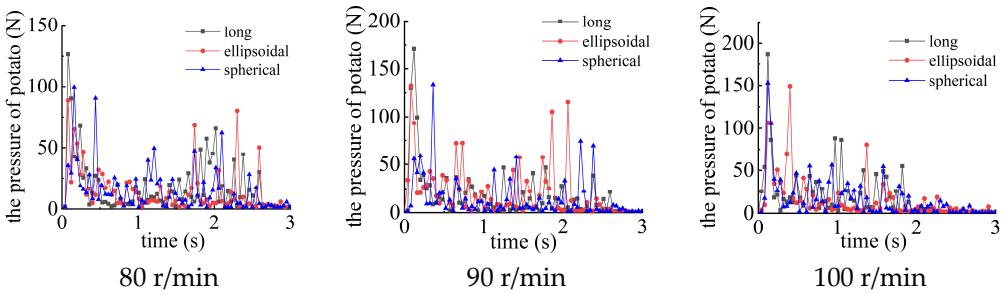

Figure 13. Mechanical characteristics of potato pieces at an inclination of the device of 6°.

As shown in Figure 13, the device inclination angle is 6°, and the separation roller speed is 80 r/min. The long-shaped potato under the three maximum pressures was 126.51 N, 89.94 N, and 67.56 N; the ellipsoidal potato under the three maximum pressures was 88.44 N, 80.10 N, 68.10 N; and the spherical potato under three maximum pressures was 99.56 N, 90.23 N, 61.93 N. It can be seen that the long-shaped potato force peak is higher than that for the ellipsoidal and spherical potatoes. This is due to the greater weight of the long-shaped potatoes. When falling from the same height, the impact force is stronger, and the collision between the long-shaped potatoes is also more substantial. When the rotation speed of the separation roller is increased to 90 r/min, the three maximum pressures endured by the long-shaped potatoes are 170.96 N, 130.02 N, and 99.32 N. The ellipsoidal and spherical shapes are 132.83 N, 115.46 N, 105.32 N and 134.03 N, 74.22 N, 69.41 N. The peak of the force occurs in the transition spacing of the separation rollers. Compared to this 80 r/min, the force is significantly higher. The rotation speed is increased to 100 r/min, the peak of the force of the long-shaped potatoes reaches 187.27 N, and the peak force of ellipsoidal and spherical potatoes is 149.10 N, 152.75 N, respectively. The force of the three kinds of potatoes is elevated when the rotational speed of the separation roller is increased, which increases with the increase in rotational speed.

Under close observation, the force diagrams of long, ellipsoidal, and spherical potatoes have five force peaks. These are the forces generated by the collision of the potato falling from the pellet factory (falling from the upper level of the potato–soil separator), the squeezing force generated by the three spacings of the four separator rollers, and the elastic deformation force generated by the potato falling from the potato–soil separator to the ground. The influencing factors are the height of the potato filling, the inclination angle of the device, the speed of the separator rollers, and the height of the potato–soil separator from the ground. The higher the height, the higher the inclination angle, and the pressure on the potato also gradually increases.

When the inclination angle of the device is 8 degrees and 10 degrees, the stress characteristics of the potato at different speeds are shown in Table 4.

Table 4. Mechanical characteristics of potatoes under different conditions (unit: N).

The Inclination Angle	The Rotation Speed	Long	Ellipsoidal	Spherical
8	80 r/min	164.14	113.48	95.55
	90 r/min	183.62	172.33	164.88
	100 r/min	204.62	207.92	191.75
10	80 r/min	113.67	103.77	114.11
	90 r/min	131.87	78.41	76.60
	100 r/min	162.49	119.58	99.28

After increasing the inclination angle of the device, ellipsoidal and spherical potatoes are smoother overall and fall more easily. The contact with the separation roller is reduced,

resulting in lower forces. In comparison, when the long-shaped potatoes have a longer axis, they do not fall as easily; their contact with the separation roller increases, leading to higher forces. As the rotational speed increased to 100 r/min, the long and ellipsoidal potato force exceeded the threshold. The friction effect and extrusion during separation are more pronounced for long-shaped and ellipsoidal potatoes with narrower rolling spaces. Spherical potatoes did not exceed the threshold, but in actual separation processes, factors such as stones can affect outcomes. Therefore, such separation conditions are no longer applicable.

When the inclination angle of the device is raised to 10° and the rotational speed of the separating roller is 80 r/min, the overall force is significantly reduced compared to lower angles, which indicates that the device's inclination angle has passed a certain threshold. When the angle is larger than this threshold, the contact friction between the three types of potatoes and the separation roller is reduced, and it is easier to roll down. The three types of potatoes completely detached from the separation roller around 2.42 s. But, under the same conditions, when the inclination angle of the device is 6° and 8°, the time for the potatoes to completely detach from the separation roller is 3.02 s and 2.75 s, respectively. Therefore, when the inclination angle of the device is too large, although the force on the potato is reduced, the movement time on the device is short. It is not able to fully remove the sticky soil by friction and collision. Similarly, the separation roller speed increased by 90 r/min and 100 r/min, and the correlation between the shape of the potato and the size of the force was weakened. The friction of the movement of the potato in the separation rollers is also reduced, resulting in a decrease in the force peak.

Combined with the three device inclinations, three separation roller speeds, and considering the three potato shapes, the following trends can be observed: As the device inclination and the separation roller speed increase, the three potato forces have an overall tendency to increase and then decrease. The potatoes continue to experience friction and rolling in during the process of removing the soil. Within a certain range of the inclination and the rotational speed of the potato, the force exerted on the potato mainly results from the force on the separation roller when it falls from the pellet factory and from the device to the ground, as well as the force generated by the separation roller squeezing it when it passes through the separation roller spacing. These forces increase with the increase in the rotational speed and the inclination angle within a certain range. But when the angle exceeds a certain threshold, the potatoes are more likely to fall on the separation roller, and the friction contact with the separation roller is reduced. If the device tilt angle is too small, it may cause blockage by preventing the potato from moving backward. Conversely, if the device tilt angle is too large, the potato may not roll sufficiently to create friction, resulting in incomplete soil removal.

In summary, under the same conditions, a larger separation roller speed should correspond to a smaller device inclination angle. The optimal combination was chosen to be a device inclination angle of 6° and a separation roller speed of 100 r/min. A smaller separation roller speed should correspond to a larger device inclination angle. The optimal combination was a device inclination angle of 8° and a separation roller speed of 80 r/min. Under these two parameter conditions, the adhering soil will be removed cleanly, and the rate of bright potato will be increased.

3.3. Effect of Separation Roller Center Distance on Potato Collision Characteristics

The diameter of the separation roller ensures that there is no leakage of potatoes; the center distance of the separation roller was initially set to 77 mm, 79 mm, and 81 mm, corresponding to the spacing of 5 mm, 7 mm, and 9 mm, respectively. The above two optimal conditions for the discrete element analysis of the potato and the device of the discrete element model are the same as the above. The test results are shown in Table 5.

Table 5. Mechanical characteristics of potatoes under different spacing (unit: N).

The Inclination Angle	The Rotation Speed	Spacing	Long	Ellipsoidal	Spherical
6	100 r/min	5 mm	147.15	140.80	128.67
		7 mm	189.81	169.41	141.13
		9 mm	201.53	194.10	181.59
8	80 r/min	5 mm	125.44	145.31	138.60
		7 mm	170.49	188.62	144.53
		9 mm	195.43	207.02	172.63

At a rotational speed of 100 r/min, with a device inclination angle of 6° and a separation of roller spacing of 5 mm, the larger diameter of the potatoes did not completely fit through the spacing. Only a small portion of the bottom contacted the gaps between the separation rollers. When the spacing increased to 7 mm, the force significantly increased, indicating that the potato had a larger contact area with the separation roller, thereby enhancing friction and extrusion. When the spacing increased to 9 mm, ellipsoidal and spherical potato forces also approached the threshold value. Therefore, the potato and the separation roller had a large area of friction contact, and the separation roller squeezing pressure exceeded the threshold value.

At a speed of 80 r/min, a device inclination angle of 8°, and a separation roller spacing of 5 mm, ellipsoidal and spherical potatoes are greater than long potatoes because these two types of potatoes are more prone to tumbling. When the pitch is 9 mm, the force of ellipsoidal potatoes exceeds the threshold.

Under the same conditions, a comparison of the force exerted by three kinds of potato under different spacing can be obtained. In a certain range, the force of three kinds of potato increases with the increase with the widening of the roller spacing. At a spacing of 9 mm, ellipsoidal potatoes have shown signs of exceeding the threshold, indicating potential skin damage and inadequate removal of the viscous soil. Therefore, a separation roller spacing of around 7 mm is considered appropriate.

3.4. Effectiveness of Clay-Heavy Soil Removal

The simulation results obtained under the above two optimal conditions are shown in Figure 14.

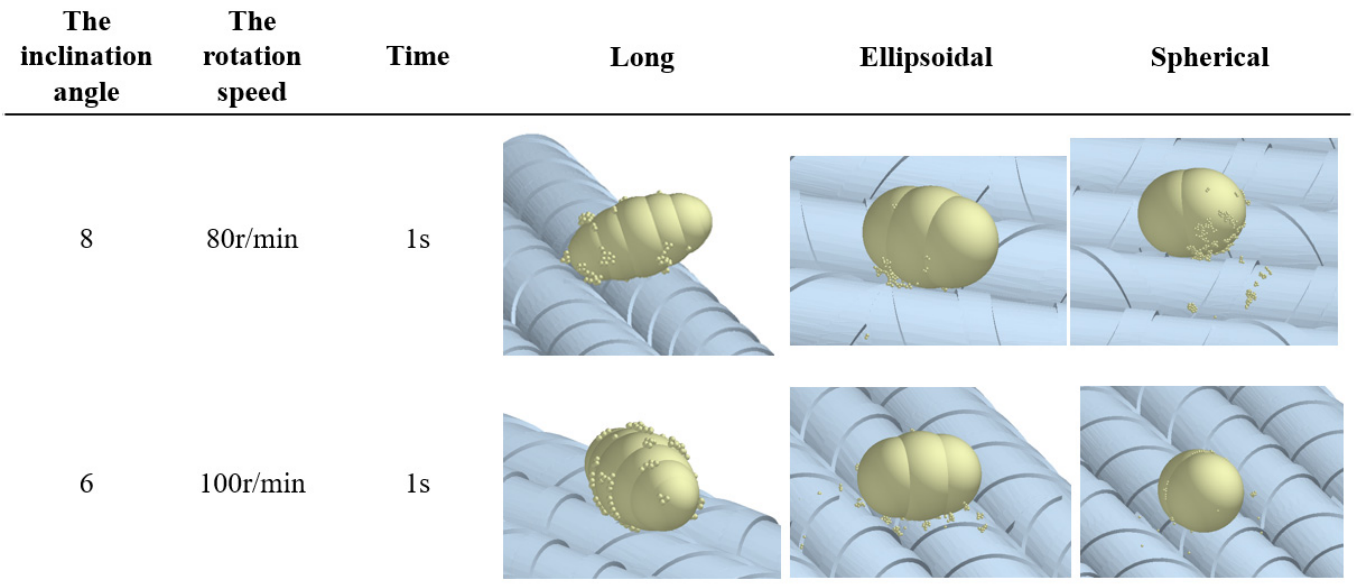

Figure 14. Removal of soil under different conditions.

Under the conditions of the device inclination angle of 8 degrees and rotational speed of 80 r/min, within the first second, the surface of the elongated potato exhibits four small aggregations of soil particles, each occupying a minimal area that barely affects the collection and transport of potatoes. In comparison, the surfaces of ellipsoid-shaped and spheroidal potatoes appear relatively cleaner. Some soil has already detached from the surface of the spheroidal potatoes. As the simulation time increases, the soil particles gradually dislodge. The ellipsoid-shaped and spheroidal potatoes tumble more effectively, enhancing the efficiency of removing the clay soil from their surfaces.

In conditions with a device inclination angle of 6 degrees and a rotational speed of 100 r/min, the situation of potato surface soil removal is similar to the previous scenario. Long potatoes, due to their shape, are more difficult to roll and experience more soil adhesion on their surfaces, whereas ellipsoidal and spherical potatoes have been cleaned more thoroughly.

3.5. Results of Field Trials

The field test process of the potato–soil separating device and the state of the post-harvest potato are shown in Figure 15.

Figure 15. Field harvest test.

When the inclination angle of the device was 6°, the rotation speed of the separation roller was 100 r/min, and the distance between the centers of the separation rollers was 79 mm. The rate of injury was 1.25%, the rate of bright potato rate was 99.01%, and the rate of skin-breaking rate was 1.58%. When the inclination angle of the device was 8°, the rotation speed of the separation rollers was 80 r/min, and the distance between the centers of the separation rollers was 79 mm. The rate of injury was 1.43%, the bright potato rate was 98.64%, and the rate of skin-breaking was 1.77%. A comparison of the performance indexes of the conventional potato–soil separation device and the potato–soil separation device designed in this paper is shown in Table 6.

Table 6. Comparison of the performances of traditional model and design model.

Model	Obvious Rate/%	Injury Rate/%	Abrasion Rate/%
Traditional model	92.21	4.92	8.45
Design model	99.01 98.64	1.25 1.43	1.58 1.77

Compared with the traditional model, the unit designed in this paper improved the rate of bright potatoes by about 6.8%, and the rate of injured potatoes and broken skins were both around 1%. The results of the comparison test are within the error tolerance, indicating that the machine's performance indicators meet the requirements for potato

harvesting. It is better suited than conventional implements for potato harvesting in sticky soil conditions.

4. Conclusions

(1) Aiming to address the issues of the high potato injury rates and low bright potato rates in traditional potato–soil separation devices, a separation roller potato–soil separation device was designed to remove the sticky soil and increase the effective separation length. A kinetic analysis of the potato–soil separation process of the separating roller was carried out, and the key factors affecting the potato–soil separation were identified.

(2) Three kinds of potatoes, Holland 15, Kexin 1, and Dry Dabai, were collected. The relationship between pressure and deformation of the three kinds of potatoes was measured using a Texture Analyzer to derive the peak force. In addition, the friction force damage of the potatoes at different heights was measured using a pressure load cell. The force threshold of the potatoes was finally determined to be 190–195 N.

(3) Three kinds of discrete element models of potato, long, ellipsoidal, and spherical, were established to study the force situation of the three kinds of potato under different separation roller speeds, center distance, and device tilt angle. The simulation analysis results showed that under the conditions of separation roller speed 100 r/min, device tilt angle 6°, separation roller center distance 79 mm and separation roller speed 80 r/min, device tilt angle 8°, and separation roller center distance 79 mm, the force on the potato did not exceed the threshold. Potato could be sufficiently tumbled and frictionless to remove the viscous soil on the separation rollers.

(4) The field test results show that the potato–soil separation device had an injury rate of 1.25%, a rate of bright potatoes of 99.01%, and a rate of broken skin of 1.58%, which meets the requirements of the potato harvester operation quality evaluation technical specifications, structural reasonableness, and adaptability. For more information on potato harvesting in sticky soil conditions, please refer to the relevant literature.

(5) The potato–soil separation unit designed in the paper is quite effective in removing clay soil, improving harvest quality, and reducing losses. The rate of bright potatoes was improved by 6.8% compared to traditional installations. The rate of potato injury and skin breakage in the installation was only about 1%. The potato–soil separation device designed in this paper can also be applied to harvesting other root crops after optimization. This study also provides new ideas for harvesting root crops in clay-heavy soil conditions.

Author Contributions: Conceptualization, X.D.; methodology, J.L. and C.Z.; software, Y.Z. and X.Z.; validation, X.D., J.L., and C.Z.; investigation, X.D. and Y.W.; resources, X.D.; data curation, X.Z. and Y.W.; writing—original draft preparation, J.L.; writing review and editing, C.Z. and Y.Z. All authors have read and agreed to the published version of the manuscript.

Funding: Longmen laboratory project (Grant No. LMFKCY2023001 and No. LMFKCY2023002), National Nature Science Foundation of China (Grant NO. 52075150), Ministry of Agriculture and Rural Affairs project (Grant NK202216050101).

Institutional Review Board Statement: Not applicable.

Data Availability Statement: The data presented in this study are available within the article.

Conflicts of Interest: The authors declare no conflicts of interest.

References

1. Khamaletdinov, R.; Martynov, V.; Mudarisov, S.; Gabitov, I.; Khasanov, E.; Pervushin, A. Substantiation of rational parameters of the root crops separator with a rotating inner separation surface. *J. Agric. Eng.* **2019**, *51*, 15–20. [CrossRef]
2. Lin, Y.; Li, S.; Duan, S.; Ye, Y.; Li, B.; Li, G.; Lyv, D.; Jin, L.; Bian, C.; Liu, J. Methodological evolution of potato yield prediction: A comprehensive review. *Front. Plant Sci.* **2023**, *14*, 1214006. [CrossRef] [PubMed]

3. Fan, J.; Li, Y.; Wang, B.; Gu, F.; Wu, F.; Yang, H.; Yu, Z.; Hu, Z. An Experimental Study of Axial Poisson's Ratio and Axial Young's Modulus Determination of Potato Stems Using Image Processing. *Agriculture* **2022**, *12*, 1026. [CrossRef]
4. Johnson, C.M.; Auat Cheein, F. Machinery for potato harvesting: A state-of-the-art review. *Front. Plant Sci.* **2023**, *14*, 1156734. [CrossRef]
5. Dorokhov, A.; Ponomarev, A.; Zernov, V.; Petukhov, S.; Aksenov, A.; Sibirev, A.; Sazonov, N.; Godyaeva, M. The Results of Laboratory Studies of the Device for Evaluation of Suitability of Potato Tubers for Mechanized Harvesting. *Appl. Sci.* **2022**, *12*, 2171. [CrossRef]
6. Ju, Y.; Sun, W.; Zhao, Z.; Wang, H.; Liu, X.; Zhang, H.; Li, H.; Simionescu, P.A. Development and Testing of a Self-Propelled Machine for Combined Potato Harvesting and Residual Plastic Film Retrieval. *Machines* **2023**, *11*, 432. [CrossRef]
7. Xin, L.; Liang, J. Design of conveyor separation device for potato harvester and analysis of its vibration characteristics. *J. Comput. Methods Sci. Eng.* **2022**, *22*, 1385–1392. [CrossRef]
8. Wang, X.; Lyu, D.; Ren, J.; Zhang, M.; Meng, P.; Li, X. Design and parameter optimization of the cleaning device for a bagged potato combine harvester. *J. Agric. Mach.* **2022**, *38*, 8–17.
9. Wei, Z.; Wang, Y.; Li, X.; Wang, J.; Su, G.; Meng, P.X.; Li, Z.H. The design and experiments of the potato combine harvester with elastic rubbing technology. *J. Agric. Mach.* **2023**, *39*, 60–69.
10. Murodov, R.K.; Nishonov, K.K.; Bayboboev, N.G.; Mamadaliev, A.M. Influence of elevator parameters with centrifugal separation on soil separation from potato tubers. In *IOP Conference Series: Earth and Environmental Science*; IOP Publishing: Bristol, UK, 2022; Volume 1112.
11. Xie, H.; Gao, G.; Tian, B.; Li, B.; Zhang, S.; Huang, J. Optimization of Potato-soil Transportation Separation Mechanism Based on Discrete Element Method and TRIZ Theory. In *Journal of Physics: Conference Series*; IOP Publishing: Bristol, UK, 2019; Volume 1267.
12. Li, H.; Gao, F. Improvement design of separation and conveying machinery and equipment of potato excavator in heavy soil. *Phys. Chem. Earth Parts A/B/C* **2023**, *130*, 103363. [CrossRef]
13. Matmurodov, F.; Dustkulov, A.; Abdiyev, N. Mathematical simulation of transfer mechanisms of crocheting potato harvesting machine. In *IOP Conference Series: Materials Science and Engineering*; IOP Publishing: Bristol, UK, 2020; Volume 883.
14. Ruzhylo, Z.; Bulgakov, V.; Adamchuk, V.; Bondarchuk, A.; Ihnatiev, Y.; Krutyakova, V.; Olt, J. Experimental research into the impact of kinematic and design parameters of a spiral potato separator on the quality of plant residues and soil separation. *J. Agric. Sci.* **2020**.
15. Wu, B.; Huang, T.; Qiu, X.; Zuo, T.; Wang, X.; Xie, F. Design and Experimental Study of Potato-Soil Separation Device for Sticky Soils Condition. *Appl. Sci.* **2021**, *11*, 10959. [CrossRef]
16. Hu, Y.; Su, M.; Wang, Y.; Cui, S.; Meng, F.; Yue, W.; Liu, Y.; Xu, C.; Yang, Z. Food production in China requires intensified measures to be consistent with national and provincial environmental boundaries. *Nat. Food* **2020**, *1*, 572–582. [CrossRef] [PubMed]
17. Li, Y.; Hu, Z.; Gu, F.; Wang, B.; Fan, J.; Yang, H.; Wu, F. DEM-MBD Coupling Simulation and Analysis of the Working Process of Soil and Tuber Separation of a Potato Combine Harvester. *Agronomy* **2022**, *12*, 1734. [CrossRef]
18. Wei, Z.; Li, H.; Sun, C.; Li, X.; Liu, W.; Su, G.; Wang, F. Improvement of potato harvester with two segments of vibration and wave separation. *J. Agric. Mach.* **2018**, *34*, 42–52.
19. Zhang, Z.; Wang, H.; Li, Y.; Yang, X.; Ibrahim, I.; Zhang, Z. Design and Experiment of Multi-stage Separation Buffer Potato Harvester. *J. Agric. Mach.* **2021**, *52*, 96–109.
20. Mosa, A.M.; Bao, G.; Wang, G.; Hu, L.; Xu, X.; Shen, H.; Ji, L. Study on the drop impact characteristics and impact damage mechanism of sweet potato tubers during harvest. *PLoS ONE* **2021**, *16*, e0255856.
21. Wei, Z.; Li, H.; Sun, C.; Su, G.; Liu, W.; Li, X. Experiments and Analysis of a Conveying Device for Soil Separation and Clod-Crushing for a Potato Harvester. *Appl. Eng. Agric.* **2019**, *35*, 987–996. [CrossRef]
22. Belay, D. Design, Construction and Performance Evaluation of Potato Harvesters: A Review. *Int. Res. J. Eng. Technol. (IRJET)* **2021**, *8*, 2747–2771.
23. Wang, L.; Liu, F.; Wang, Q.; Zhou, J.; Fan, X.; Li, J.; Zhao, X.; Xie, S. Design of a Spring-Finger Potato Picker and an Experimental Study of Its Picking Performance. *Agriculture* **2023**, *13*, 945. [CrossRef]
24. Chen, M.; Liu, X.; Hu, P.; Zhai, X.; Han, Z.; Shi, Y.; Zhu, W.; Wang, D.; He, X.; Shang, S. Study on rotor vibration potato-soil separation device for potato harvester using DEM-MBD coupling simulation. *Comput. Electron. Agric.* **2024**, *218*, 0168–1699. [CrossRef]
25. Li, J. *Study and Optimum Design on Separation and Screening Performance of Potato and Soil of Potato Harvester*; Inner Mongolia Agricultural University: Huhhot, China, 2019.
26. Jia, B.; Sun, W.; Zhao, Z.; Wang, H.; Zhang, H.; Liu, X.; Li, H. Design and Field Test of a Remotely Controlled Self-Propelled Potato Harvester with Manual Sorting Platform. *Am. J. Potato Res.* **2023**, *100*, 193–209. [CrossRef]
27. Li, Y.; Fan, J.; Hu, Z.; Luo, W.; Yang, H.; Shi, L.; Wu, F. Calibration of Discrete Element Model Parameters of Soil around Tubers during Potato Harvesting Period. *Agriculture* **2022**, *12*, 1475. [CrossRef]
28. Mu, G.; Wang, W.; Zhang, T.; Hu, L.; Zheng, W.; Zhang, W. Design and Experiment with a Double-Roller Sweet Potato Vine Harvester. *Agriculture* **2022**, *12*, 1559. [CrossRef]
29. Gangopadhyay, M.; Zhao, P.; Tian, Y.; Li, Y.; Xu, G.; Tian, S.; Huang, Z. Potato (*Solanum tuberosum* L.) tuber-root modeling method based on physical properties. *PLoS ONE* **2020**, *15*, e0239093.

30. Wei, Z.; Su, G.; Li, X.; Wang, F.; Sun, C.; Meng, P. Parameter optimization and Test of Potato Harvester Wavy Sieve Based on EDEM. *Agric. Mach* **2020**, *51*, 109–122.
31. *NY/T 648-2015*; Technical Specification for Quality Evaluation of Potato Harvesters. China Standard Press: Beijing, China, 2015.